Automatic Reaction Network Generation using RMG for Steam Cracking of n-Hexane

Kevin M. Van Geem, Marie-Francoise Reyniers, and Guy B. Marin
Laboratorium voor Petrochemische Techniek, UGent, Krijgslaan 281 (S5) B-9000 Gent, Belgium

Jing Song and William H. Green
Dept. of Chemical Engineering, Massachusetts Institute of Technology, Cambridge, MA 02139

David M. Matheu
National Institute of Standards and Technology, Gaithersburg, MD 20899

DOI 10.1002/aic.10655
Published online October 12, 2005 in Wiley InterScience (www.interscience.wiley.com).

A new reaction mechanism generator RMG is used to automatically construct a pressure dependent kinetic model for the steam cracking of n-hexane. Comparison between simulated and pilot plant data shows that RMG is able to generate detailed reaction networks that accurately predict the conversion and the yields of the major products although none of the kinetic parameters are fit to the experiments. RMG generates reaction networks based on minimal assumptions, making it possible to test commonly used assumptions such as the μ-hypothesis and the quasi steady-state approximation (QSSA) for μ-radicals, traditionally used in steam cracking,[1,2] as well as in pyrolysis.[3] The RMG-reaction network for n-hexane confirms that no bimolecular reactions of heavy radical species are important at the examined conditions (COT: 953 K - 1090 K; COP: 0.20 MPa -0.24 MPa; <80% conversion), and that the QSSA for the group of μ-radicals leads to negligible errors. RMG also offers the possibility to estimate the error introduced by neglecting the pressure dependence of most of the reactions. In the case studied, this frequently made (but seldom tested) approximation appears to be justified. © 2005 American Institute of Chemical Engineers *AIChE J,* 52: 718–730, 2006
Keywords: steam cracking, reaction network generation, pressure dependence, sensitivity analysis

Introduction

Large-scale detailed kinetic models find increasing use in the modeling of combustion processes, atmospheric chemistry, soot formation, and other areas of industrial or environmental interest. Because such reaction networks may contain up to thousands of reactions and species, constructing them by hand can be tedious and error-prone. Therefore, many research groups have developed computer tools to automatically generate these mechanisms.[2,4,5,6,7,8,9,10,11,12,13,14,15,16] A key difficulty with mechanism generation programs is that they can be combinatorial, producing large numbers of kinetically unimportant reactions and species. Moreover, sometimes nonphysicochemical criteria and/or expert user involvement are employed to limit mechanism growth, thereby risking the possibility that important reactions are not included. In contrast, rate-based termination of computer-generated reaction mechanisms provides a physicochemical criterion for including reactions and

Current address of D. M. Matheu: Cabot Corporation, 157 Concord Rd., Billerica, MA 01821.
Correspondence concerning this article should be addressed to K. M. Van Geem at kevin.vangeem@ugent.be

species,[12,17,18] only those pathways whose flux exceeds some minimum flux criterion R_{min} are included in the network. XMG (Exxon-Mobil Mechanism Generator) was the first network generation software applying the rate based termination criteria[14] and is based on the NETGEN code developed by Klein and coworkers.[12] XMG has been further elaborated, adding several new features. Matheu et al.[19,20] created XMG-Pdep, the first mechanism generator to systematically include pressure-dependent reactions. Recently, RMG, a new mechanism generator, belonging to the same family, has been developed.[21] RMG includes XMG-PDep's capabilities but also features the implementation of advanced technologies, such as graph representation of reaction families and a hierarchical tree-structured database for retrieving thermal and kinetics parameters, and the use of object-oriented technology. These changes strongly facilitate to continuously improve the level of detail in the description of the chemistry as compared with prior network generation software.[22]

An accurate prediction of the conversions and yields would greatly enhance not only the design of steam-cracking or pyrolysis units but would also provide a practical tool to determine the optimal operation conditions and/or to evaluate the process economy as a function of feedstock composition. Historically, it was infeasible to accurately determine all of the parameters in large chemical kinetic models *a priori*, so developing accurate models involved fitting to a vast number of experimental data and required extensive and time-consuming experimental work to gather the necessary data. At present, estimation methods, particularly those based on quantum chemistry, have significantly improved, allowing a reliable *a priori* determination of kinetic and thermodynamic data. In this work we assess the performance of these improved rate estimation methods, as implemented in RMG, to predict the yields obtained during steam-cracking of n-hexane in a pilot plant (located at the "Laboratorium voor Petrochemishe Techniek" (LPT) of Gent University) for which a good correlation with full scale industrial units was shown previously.[23,24]

The accuracy of the kinetic parameters used to construct the models is of the utmost importance, especially when using a rate based termination criterion, as the rate estimates determine whether or not an elementary step will be included in the final mechanism. Certain reaction pathways can indeed remain unidentified because the kinetic parameters are inaccurate or because the model generator omitted some reaction families, leading to incomplete reaction networks. Adjustment of the kinetic parameters of an incomplete reaction network to impose agreement with experimental data then forces some of the reactions in the model to take over the roles of the unidentified reactions, thereby reducing the physicochemical basis of the model and hence restricting its valid range of extrapolation.

Several assumptions are commonly made in models for steam cracking and pyrolysis. The first assumption usually made is the μ-radical hypothesis.[1,2,3] This assumption states that for large radicals bimolecular reactions can be neglected. These large radicals are called μ-radicals or radicals having a μ-character since, in the model, their reaction possibilities are restricted to monomolecular reactions only. In steam cracking, radicals containing more than 5 carbon atoms are traditionally considered μ-radicals.[2] RMG does not consider the assumption of the existence of μ-radicals *a priori*, hence, the generated reaction mechanism for n-hexane can be used to test the μ-radical hypothesis.

Other commonly made assumptions are the long-chain hypothesis, allowing a partial separation of the fast propagation reactions from the slower initiation/termination reaction,[25,26] and the quasi-steady-state approximation (QSSA) for the concentration of some reactive intermediates.[5] Careful use of both these assumptions can simplify the solution of the kinetic equations considerably. None of these assumptions is made *a priori* in RMG — the complete set of kinetic equations is integrated using a stiff solver. RMG thus provides the possibility to validate these frequently used approximations.

Finally, all previous models for naphtha steam-cracking have assumed that the rates of most of the scission and addition reactions are in the high-pressure-limit. Most modern models account, at least implicitly, for the fall-off behavior of a handful of reactions of atoms and very small molecules; here the issue is whether or not it is necessary to consider pressure-dependence for the many reactions of large polyatomics. Recent work has indicated that some reactions of even large molecules and radicals proceed via pressure-dependent pathways,[27] with steam cracking lying in the P,T region where a transition from the high-pressure limit to pressure-dependent behavior can be expected. Dean[28] showed the use of pressure-dependent kinetic parameters is important for the pyrolysis of methane, as it introduces fast pathways to form C5 ring species, thereby significantly altering the overall kinetics. The importance of including pressure dependent pathways for polyatomics was further illustrated for high-conversion ethane pyrolysis,[29,30] methane autocatalysis and high-conversion ethane pyrolysis.[20] The new mechanism generator RMG allows evaluation of the overall effect of pressure dependence on the simulated yields. The use of the RMG software package to study the behavior of a model compound for naphtha feedstocks, such as n-hexane, can lead to new insight in this matter.

Experimental

The steam cracking of n-hexane was studied in the LPT pilot plant.[31] This experimental setup allows measurement of the kinetics of the cracking reactions,[32] and of the coke deposition in both the radiant coil[33] and the transfer line exchanger (TLE).[34] n-Hexane is selected as feedstock because it is an excellent model compound for the cracking behavior of light naphtha fractions. Naphtha feedstock molecules typically have a carbon number in the range from 5 to 10 and are mostly paraffinic or iso-paraffinic in nature. A representation of the pilot plant installation is given in Figure 1. The furnace is divided into seven separate cells that can be fired independently, allowing to set a broad range of temperature profiles in the reactor coil. Ninety premixed side-wall burners are arranged to make the heat distribution more uniform in a cell.[35] Water and the hydrocarbon feedstock are fed separately, preheated and mixed in the first 2 cells. The reaction section of the tube extends from cell 3 to cell 7, and is 12.4 m long and has an internal dia. of 9 mm. These dimensions are chosen to achieve turbulent flow conditions in the reactor coil suspended in the furnace. The temperature and pressure profiles along the tube are measured and the outlet pressure can be regulated. The pilot plant includes an extended on-line analysis section pro-

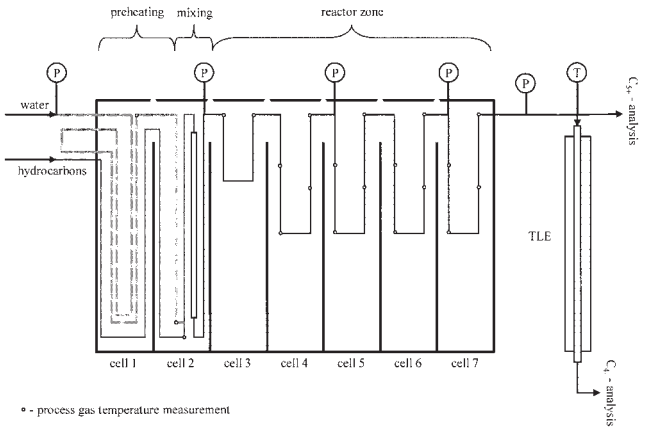

Figure 1. The preheating, mixing and reactor section of the LPT pilot plant installation.

[(P): pressure measurement, (T): process gas temperature measurement].

viding a product distribution ranging from C1 to C18 (bp ~ 400°C) including H_2, CO, and CO_2.

The experimental conditions used in this work are summarized in Table 1. The flow rate of the hydrocarbon feedstock is varied from 3 kg h^{-1} to 4kg h^{-1}, while the coil outlet temperature (COT) varies from 953 K to 1075 K. The dilution is kept at a fixed value of 0.4 $kg_{steam}/kg_{hydrocarbons}$. The coil inlet pressure (CIP) varies from 0.24 MPa to 0.28 MPa. The coil outlet pressure (COP) varies from 0.20 MPa to 0.24 MPa. These conditions correspond with hexane conversions ranging from 25 to 75%.

Automatic mechanism generation with integrated pressure dependence

RMG uses a set of "reaction families" to generate all possible reactions that a given chemical species can undergo as such and in the presence of the other species in the mechanism. Each reaction family represents a particular type of elementary chemical reaction, such as bond-breaking, or radical addition to a double bond. Currently, thirty-three primary reaction families are defined; this is the richest set of reaction families ever compiled. RMG represents the individual chemical species as a 2-dimensional (2-D) connectivity graph and defines the possible reactions by considering the possible mutations of the graph. The newly formed species are then considered as candidates for further reactions, and their reactions can be added to RMG's chemical kinetic model.

As with most mechanism generation tools, RMG obtains the necessary thermochemical data from an electronic database of literature values whenever possible. In most instances, however, it must resort to group contribution methods to estimate enthalpies of formation, heat capacities, entropies, and certain other data required for modeling pressure-dependent reactions. In this work, literature thermochemistry data were taken from the database assembled by Wijaya[36] and the group contribution package of Song and coworkers,[22] embedded in RMG, was used to obtain estimates whenever literature values were not available. The group contribution values used were taken from Benson,[37] from Lay[38] and from Sumathi.[39,40,41] The values for the thermodynamic properties obtained at different temperatures are used to fit the coefficients of the NASA polynomials used in CHEMKIN.[42]

Similarly, RMG draws rate constant information from a library of literature-based kinetic rate constants whenever these are available, as in Matheu et al.[20] For the vast majority of RMG-determined reaction possibilities, no values are available, and the algorithm thus uses a large set of so called "rate rules" stored in a kinetics database to estimate the rate constants for each reaction. The rate rule database contains mainly high-level quantum chemistry calculation results from Sumathi et al.[39,41,43,44], from Wijaya et al.[45] and from Saeys et al.,[46] and rate estimates from the Livermore group.[47] If the reaction is pressure-dependent, the rate rule is a "high-pressure-limit" rate rule and serves as an input to a CHEMDIS calculation[48] of k(T,P).[49] Based on Matheu's work[29] we also added a set of net pressure-dependent reactions which reflect the propargyl + propargyl network, and its associated isomerizations, from the results of Miller and Klippenstein.[50]

RMG considers every reaction of the form A + B → C, B → C, or B → C + D to initiate a partial pressure-dependent reaction network, such as those described in Matheu et al.[49] During mechanism generation, RMG builds a set of these partial pressure-dependent networks, and from these, it constructs net pressure-dependent reactions and estimates their rate constants $k(T,P)$. Each partial pressure-dependent network is explored by only one activated isomer at a time. The algorithm is named the "Activated Species Algorithm", or ASA, since it stores chemically or thermally activated species as they were distinct species. Like many mechanism generators, it maintains a pool of Reacted Species, whose pathways in the pressure-dependent network have been explored, and a pool of Unreacted Species have been discovered, but not yet explored. For each partial network, RMG uses the QRRK/MSC code CHEMDIS to estimate the $k(T,P)$ values of every net pressure-dependent reaction. It also examines the maximum flux to all non-included portions of the partial pressure-dependent network, the so-called "leakage" flux $R_{leak(i)}$ for a partial network i. If this flux is greater than the cutoff flux, the partial network is "grown" by one isomer, with all its high-pressure-limit elementary steps and $R_{leak(i)}$ decreases because an activated isomer is added to the network. The growth of each partial pressure-dependent network is halted when the flux to non-included portions is less than the cutoff flux. In this way pressure-dependent reactions can be included systematically and rationally.

RMG periodically constructs a set of ordinary differential equations (ODEs) representing the evolution of the system described by its current mechanism. At each time step, it calculates the flux $R_{species(j)}$ to each candidate species that it has not yet included in the mechanism; j runs over all possible candidates for inclusion. It also evaluates each leakage flux

Table 1. Experimental Conditions Used for the Cracking of *n*-Hexane in the LPT Pilot Plant Installation

CIP (MPa)	0.24–0.28
COP (MPa)	0.20–0.24
CIT (K)	873
COT (K)	953–1075
Dilution ($kg_{steam}/kg_{Hydrocarbon}$)	0.4
Hydrocarbon flow rate (kg/h)	3.0–4.0
Conversion (%)	25–75

Table 2. Effect of the Input Values (Error Tolerance f_{min} and Conversion) on the Size of the Reaction Network and on the Number of Species in the Reaction Network [both Considered and Included Reactions and Species]

	Considered Species	Considered Reactions	Included Species	Included Reactions
Error Tolerance: 0.01 Conversion: 0.5	147	513	19	194
Error Tolerance: 0.005 Conversion: 0.2	541	1660	33	616
Error Tolerance: 0.005 Conversion: 0.5	2121	6219	60	1178

Reaction networks generated at a pressure of 0.22 MPa, a temperature of 1025 K, and initial *n*-hexane concentration of 10^{-6} mol m^{-3}.

$R_{leak(i)}$, where i runs over all partial pressure-dependent networks. RMG selects that species or pressure-dependent network having the largest flux and explores its reactions, adding the species and/or reactions to the kinetic model. The process is "complete" when RMG can solve the ordinary differential equations to a user-specified conversion, with all fluxes to nonincluded parts of the mechanism less than the scaled flux criterion R_{min}, over the entire integration time t. The flux criterion R_{min} is given by

$$R_{\min}(t) = f_{\min} R_{\text{char}}(t) \tag{1}$$

$R_{char}(t)$ is the characteristic rate for the whole mechanism at time t, as given by Song et al.[21]

$$R_{\text{char}}(t) = \sqrt{\sum_j R^2_{\text{reacted}(j)}(t)} \tag{2}$$

and f_{min} is a user-specified tolerance, typically 0.1–1%. $R_{reacted(j)}(t)$ represents the net rate of change of each species present in the mechanism at time t.

To build the ordinary differential equations required during mechanism generation, RMG must implicitly assume a reactor model. RMG uses a very simple, perfectly-mixed batch reactor model, at constant temperature and pressure. Hence, RMG as such cannot simulate an experiment performed in the LPT pilot plant, as the reactor used in the pilot plant is a tubular reactor exhibiting an axial temperature and pressure profile. This shortcoming is circumvented by combining the RMG-generated mechanism at constant temperature and pressure with CHEMKIN.[42] CHEMKIN'S PLUG tool solves the set of differential equations describing an arbitrary-geometry plug-flow reactor using the implicit numerical software DASSL.[51] The temperature and pressure profile used in PLUG are taken from the corresponding pilot plant experiment. Matheu et al.[29] used a similar strategy for modeling a set of ethane pyrolysis experiments. However, combining CHEMKIN with the RMG generated mechanism is not straightforward; altering the input values used to generate the reaction network with RMG influences the size, the number of included species and the kinetics of the reaction network. Special care has to be taken as to which values are used to generate the reaction network; in particular, the choice of the temperature and pressure can noticeably affect the details of the model predictions. As the actual pressure drop in the pilot plant set-up is quite small (0.04 MPa, <20% CIP), it is not surprising that the use of a fixed pressure in RMG to generate the reaction network does not affect the number of included species and the kinetics of the reaction network. The isothermal approximation in the reactor clearly could be a much more important source of error. However, we observed that, if the highest temperature of the corresponding pilot plant experiment (in this case ± 1,075 K) is chosen, a model is generated which includes all the species and reactions that are important over the whole T range. The problem of estimating the range of conditions over which an automatically-generated reaction mechanism is valid has been discussed previously by Song et al.[57]

Another technical but important issue concerns the transformation of pressure dependent reactions into the appropriate CHEMKIN format.[42] In this work, a modified Arrhenius format, as presented by Dean et al.[28] has been used. The QRRK code CHEMDIS[48] is used in this work to fit modified Arrhenius forms to $k(T,P)$ values at constant pressure over a limited temperature range, as demonstrated previously by Dean.[28] CHEMDIS and THERFIT[53] provide estimates of the rate constants k(T,P) for pressure dependent reactions, using the rate rules as input. The fitted Arrhenius parameters for $k(T,P)$ have no physical meaning and are specific for a given pressure, but as a fitting form they allow accurate reproduction of calculated $k(T,P)$ values in the temperature and pressure range considered in this work. This representation allows RMG to represent its mechanism in a suitable CHEMKIN input file, using "pressure-dependent" rate constants that are valid for one particular pressure but spanning a temperature range. In this work, a model generated at P = 0.21 MPa was used and compared with a model generated using the high-pressure limit values for the rate constant (P→∞).

As stated earlier, the experiments performed in the pilot plant reactor are modeled using CHEMKIN's PLUG utility.[42] Assuming a 1-D reactor model, as in PLUG, to model the steam cracking process can lead to errors, such as when modeling ethane cracking in a Lummus SRT-I reactor.[54] The source of these errors is that in industrial single coil reactors for ethane cracking important radial temperature gradients (>100 K) exist (d = 100 mm).[54] As the tube diameter in the pilot plant reactor used in this work is much smaller (that is, d = 10 mm), the radial temperature gradients are far less pronounced (< 15 K), thereby allowing a reasonable accurate simulation using a 1-D reactor model.

Results

Reaction network and simulation results

The size and the number of species considered and included in the reaction network depend mainly on the conversion level and the user-defined tolerance f_{min}. In Table 2 the number of species and reactions considered and ultimately included in the

Table 3. Simulated Conversion and Product Yields for *n*-Hexane Steam Cracking

	Full Mechanism (wt%)	Reduced Mechanism (wt%)	Experimental Results (wt%)
H_2-yield	0.4	0.6	0.4
CH_4-yield	6.0	5.5	5.6
C_2H_2-yield	0.2	0.2	0.3
C_2H_4-yield	19.0	21.2	19.3
C_2H_6-yield	2.7	2.1	3.3
C_3H_4-yield	0.2	0.5	0.2
C_3H_6-yield	10.4	11.6	10.8
C_4H_6-yield	4.4	5.0	2.7
1-C_4H_8-yield	4.4	3.6	5.8
2-C_4H_8-yield	1.8	1.6	0.4
1-C_5H_{10}-yield	1.1	1.9	2.2
C_6H_6-yield	0.0	0.0	0.1
C_6H_{14}-conversion	50.9	53.8	51.5

Full mechanism of 60 species and 1178 reactions: reaction network generated with RMG at a pressure of 0.22 MPa, a temperature of 1025 K, an initial *n*-hexane concentration of 10^{-6} mol m^{-3}, a user-defined tolerance of 0.005, and a conversion set at 50%. Reduced mechanism of 24 species and 56 reactions: from full mechanism using combination of sensitivity analysis and rate of production analysis [simulation conditions: CIT = 873 K, COT = 997 K, CIP = 0.27 MPa, COP = 0.24 MPa; F: 4.0 kg h^{-1}, δ = 0.4 kg/kg].

reaction network are given for different conversion levels and user-defined tolerances. Obviously, lower tolerances and higher conversion levels lead to larger reaction networks. At 0.22 MPa, 1,025 K, an initial n-hexane concentration of 10^{-6} mol m^{-3}, a user-defined tolerance $f_{min} = 0.005$, and a conversion set at 50%, the generated reaction network consists of 60 species and 1,178 reactions, while RMG considered 2,121 species and 6,219 reactions. The generated reaction mechanism consists of 20 C-C and C-H scission reactions of molecules and their reverse reactions, 432 hydrogen abstractions, 32 hydrogen migrations, 512 disproportionations (and their reverse reactions), 81 additions and the corresponding 81 β-scissions. For these conditions, all the major and minor products observed in the pilot plant experiment are included in the reaction network: n-hexane, hydrogen, methane, acetylene, ethylene, ethane, methyl acetylene, propadiene, propylene, butadiene, 1-butene, 2-butene and 1-pentene. The use of tighter tolerances significantly increases the size of the model, but does not significantly affect the model predictions.

The RMG reaction network was then used to simulate 10 pilot plant experiments. These are pure predictions, that is, no parameters were adjusted to fit the experimental data. The simulation results are compared with the experimental data in Table 3. A good agreement between simulation results and experimental data for the main reaction products was obtained. The yields for the minor products 2-butene, 1-pentene and butadiene deviate significantly from the experimentally observed yields. In Figure 2 a parity plot for the conversion is given, while in Figure 3 the parity plot for the major products (methane, ethylene and propylene) is shown. Even under severe cracking conditions, the conversion and the yields of the main products are accurately simulated. In Figure 4 the parity plot for ethane, 1-butene, butadiene and 1-pentene is shown. These results illustrate that although for the minor products the simulation results are reasonable, significant deviations for the yields of 1-butene, butadiene and 1-pentene, especially at higher conversions, occur.

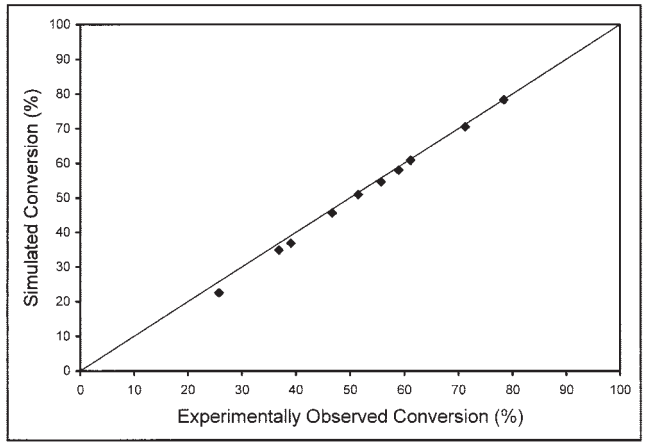

Figure 2. Parity plot for the conversion of n-hexane simulated with the full mechanism considering 60 species and 1,178 reactions.

[Simulation Conditions: CIT = 873 K; COT: 953 K – 1090 K; CIP: 0.26 – 0.28 MPa; COP: 0.22 MPa -0.24 MPa; F: 3.0 – 4.0 kg h^{-1}; δ = 0.4 kg/kg].

Reaction network reduction and analysis

In this article, we have used the combination of sensitivity analysis[55,56] and rate of production analysis[57] to reduce the generated mechanism to its most important reactions.[58,59,60,61] CHEMKIN 4.0[42] is used to calculate the sensitivity coefficients and the production rates of the species. In agreement with Brock et al.[59] reactions are included in the skeletal mechanism if the sensitivity coefficients are higher than 0.1, or if the net rate is higher than 5% of the net rate of the fastest step in the considered time interval. The full reaction network consisting of 1,178 reactions can then be reduced to 55 reactions.

The reduced mechanism presented in Table 4 is able to capture the main trends of the full mechanism. Indeed, the simulation results obtained using the reduced network (see Table 3) illustrate that the reduced mechanism is perfectly able

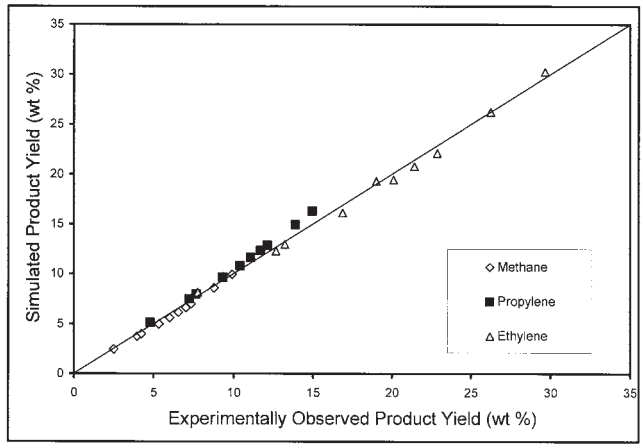

Figure 3. Parity plot for the yields of methane, ethylene and propylene with the full mechanism considering 60 species and 1,178 reactions.

[Simulation Conditions: CIT = 873 K; COT: 953 K – 1090 K; CIP: 0.26 – 0.28 MPa; COP: 0.22 MPa -0.24 MPa; F: 3.0 – 4.0 kg h^{-1}; δ = 0.4 kg/kg].

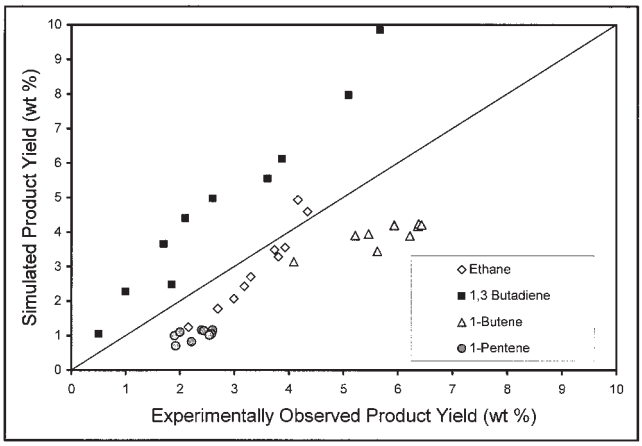

Figure 4. Parity plot for the yields of ethane, 1-butene, butadiene and 1-pentene with the Full Mechanism considering 60 species and 1178 reactions.

[Simulation Conditions: CIT = 873 K; COT: 953 K – 1090 K; CIP: 0.26 – 0.28 MPa; COP: 0.22 MPa -0.24 MPa; F: 3.0 – 4.0 kg h^{-1}; δ = 0.4 kg/kg].

to simulate the n-hexane experiments with only a minor loss of accuracy as compared to the full mechanism. This clearly shows that although the rate-based algorithm leads to more compact mechanisms than some other reaction mechanism generation strategies, a large number of kinetically unimportant reactions are still included in the full mechanism. Note that the kinetic parameters in Table 4 correspond to the high-pressure limit values for the forward reactions and that all forward reactions are endothermic. Reporting the fitted Arrhenius parameters from fitting k(T,P) at a fixed P would only cause confusion because those values have no physical meaning and are particular to a specific pressure and narrow temperature range. The kinetics for the reverse exothermic reactions are calculated based on the thermochemistry and the values of the forward endothermic reactions.

The reduced mechanism in Table 4 suggests that hydrogen migration reactions and disproportionation reactions are of limited importance. Only one hydrogen migration reaction is included in the skeletal mechanism, while only four disproportionation reactions out of the 512 disproportionation reactions originally present in the full mechanism remain present in the compact mechanism. Many pyrolysis/steam-cracking models completely neglect unimolecular hydrogen migration reactions and bimolecular radical-radical disproportionation reactions while others lump isomeric radicals together, implicitly assuming that unimolecular H-migration is equilibrated. Here we test whether these reaction families are indeed negligible under steam-cracking conditions. The results in Table 5 show that these two reaction families do not play an important role under the specified conditions. Especially the disproportionation reactions are of no importance. The yields of the major and minor products remain practically unchanged when disproportionations are not considered in the reaction network. This is in sharp contrast to what is observed in autocatalytic methane pyrolysis,[20] where the reverse of the disproportionation reactions is a significant source of radicals. Unimolecular hydrogen migration reactions are not entirely negligible in naphtha steam cracking. Removing this reaction family completely from the network results in a small shift from ethylene to propylene along with a significant shift from 2-butene to 1-butene.

The results of the rate of production analysis can give an indication of the local importance of a reaction. Some reactions, such as the C-C scissions of n-hexane, are very important at short axial distances in the tubular reactor for converting n-hexane (see Figure 5). Other reactions, such as the hydrogen abstraction reactions from n-hexane, are less important in the early stages of the reactor but gain in importance toward the reactor outlet. A sensitivity analysis was manually performed by simultaneous variation of the forward and the reverse rate constants for the elementary steps in order to ensure thermodynamic consistency. The rate rules for the scission reactions were found to be most critical for the agreement with experimental data. Multiplying all of the rate rules in the kinetic database for scission reactions with a factor 10 prior to generation strongly affects the simulated product distribution. The built-in thermodynamic consistency incorporated in RMG makes that the recombination rate rules, combined with the assumed thermochemistry, determine the kinetic parameters of the corresponding reverse reactions, that is, the C-C scissions of the n-hexane molecules; narrowing the uncertainties in both the recombination rate estimates and in the thermochemistry estimates could further improve the accuracy of the predictions. The model predictions are less sensitive to the rate constants of the bimolecular H-abstraction reactions, the key propagation step in the process.

The results of the rate of production analysis also allow for an easy identification of the important reaction pathways. For example, the bar plot for the production rates of ethylene in Figure 6 shows that most of the ethylene is produced via the β-scission of the ethyl radical

$$C_2H_5^{\bullet} \Leftrightarrow C_2H_4 + H^{\bullet} \tag{3}$$

Other reactions contributing significantly to the ethylene production are the β-scissions of the primary hexyl radicals and the primary propyl radicals. The β-scissions of the primary butyl radicals contribute to the ethylene production to a lesser extent.

Identifying the important pathways to propylene is not as straightforward as for ethylene. Only the balanced system of addition reactions, β-scission reactions and hydrogen abstractions can explain the propylene behavior.[60] The rate of production analysis shows that the β-scission of the 2-hexyl radicals is the most important reaction for propylene formation

$$C_6H_{13}^{\bullet}(2) \Leftrightarrow C_3H_6 + C_3H_7^{\bullet} \tag{4}$$

Other minor paths that contribute significantly to the formation of propylene are the C-H β-scission of the secondary propyl radical and the β-scission of the secondary butyl radical. The rate of production analysis shows that a set of hydrogen abstractions involving allylic radicals are also important for an accurate prediction of the propylene yield, for example, the hydrogen abstractions from ethylene

$$C_2H_4 + C_3H_5^{\bullet}(al) \Leftrightarrow C_3H_6 + C_2H_3^{\bullet} \tag{5}$$

Table 4. Skeletal Mechanism: Reduction via the Combination of Sensitivity Analysis and Rate of Production Analysis

Reaction	log(A)	n	E_a
C–C Scission and Recombination			
C6H14 ↔ C3H7•(1) + C3H7•(1)	23.5	−2.0	369
C6H14 ↔ C4H9•(1) + C2H5•	23.2	−1.9	369
C6H14 ↔ C5H11• + CH3•	21.4	−1.4	374
C2H6 ↔ CH3• + CH3•	23.9	−2.2	384
Hydrogen Abstraction			
C6H14 + C4H7(1)• ↔ C6H13•(3) + 1-C4H8	12.3	0.5	99
C6H14 + C4H7(1)• ↔ C6H13•(2) + 1-C4H8	12	0.7	99
C6H14 + C4H7(1)• ↔ C6H13•(1) + 1-C4H8	9.5	1.4	108
C6H14 + C4H7(1)• ↔ C6H13•(3) + 2-C4H8	17.8	−1.4	98
C6H14 + C4H7(1)• ↔ C6H13•(2) + 2-C4H8	17.3	−1.2	98
C6H14 + C4H7(1)• ↔ C6H13•(1) + 2-C4H8	15.3	−0.6	108
C6H14 + C3H5• ↔ C6H13•(3) + C3H6	17.9	−1.4	98
C6H14 + C3H5• ↔ C6H13•(2) + C3H6	17.4	−1.2	98
C6H14 + C3H5• ↔ C6H13•(1) + C3H6	15.5	−0.6	108
C3H4 + C4H7(1)• ↔ C3H3• + 1-C4H8	14.2	0	129
C2H6 + C6H13•(3) ↔ C2H6• + C6H14	8.6	0.9	61
C2H6 + C6H13•(2) ↔ C2H6• + C6H14	9.2	0.7	62
C2H6 + C6H13•(1) ↔ C2H6• + C6H14	11.8	0	62
C2H6 + C4H7•(1) ↔ 1-C4H8 + C6H14	9.3	1.4	108
C2H4 + C6H13•(1) ↔ C2H3• + C6H14	12.5	0.2	80
C2H4 + CH3• ↔ C2H3• + CH4	16.1	−0.3	84
C2H4 + C3H5• ↔ C3H6 + C2H3•	15.9	−0.4	129
CH4 + C5H9• ↔ CH3• + C5H10	14.3	0.1	126
CH4 + C6H13•(1) ↔ CH3• + C6H14	4.1	2.4	61
CH4 + C6H13•(2) ↔ CH3• + C6H14	2.4	2.9	60
CH4 + C6H13•(3) ↔ CH3• + C6H1	2.0	3.1	60
CH4 + C4H7•(1) ↔ 1-C4H8 + CH3•	14.4	0.2	126
CH4 + C4H7•(1) ↔ 2-C4H8 + CH3·	15.2	−0.5	108
H2 + C6H13•(2) ↔ H• + C6H14	3.4	2.6	41
H2 + C6H13•(3) ↔ H• + C6H14	5.5	2.1	43
Hydrogen Abstraction			
H2 + C6H13•(1) ↔ H• + C6H14	3.1	2.8	40
H2 + C4H7•(1) → 2-C4H8 + H•	6.5	2.1	79
H2 + C4H7•(1) → 1-C4H8 + H•	5.9	2.4	84
H2 + C3H5• ↔ H• + C3H6	6.5	2.1	79
H2 + CH3• → H• + CH4	7.2	1.7	41
Beta–Scission and Addition			
C6H13•(3) ↔ CH3• + C5H10	17.3	−0.6	142
C6H13•(3) ↔ C2H5• + 1-C4H8	19.5	−1.2	142
C6H13•(2) ↔ C3H7•(1) + C3H6	20.3	−1.5	142
C6H13•(1) ↔ C4H9•(1) + C2H4	21.7	−1.9	144
C5H11• ↔ C3H7•(1) + C2H4	21.7	−1.9	144
C5H11• ↔ C2H5•(1) + C3H6	20.1	−1.4	142
C5H11• ↔ H• + C5H10	13	0.1	153
C5H9• ↔ CH3• + C4H6	19.2	−1.2	171
C4H9•(1) ↔ C2H5• + C2H4	21.5	−1.8	144
C4H9•(2) ↔ CH3• + C3H6	16.9	−0.9	142
C4H9•(2) ↔ H• + 2-C4H8	11.3	0.4	147
C4H9•(2) ↔ H• + 1-C4H8	11.0	0.7	155
C4H7•(v) ↔ CH3• + C3H4	17.8	−0.9	150
C4H7•(1) ↔ C2H3• + C2H4	18.4	−1.5	173
C3H7•(1) ↔ CH3• + C2H4	18.6	−1.3	145
C3H7•(1) ↔ C3H6 + H•	12.1	0.5	155
C2H5• ↔ H• + C2H4	13.3	0.2	160
C2H3• ↔ H• + C2H2	12.1	0.6	157
Hydrogen Migration			
C6H13•(2) ↔ C6H13•(1)	8.3	0	69
Disproportionation (Reverse & Forward)			
C4H6 + 1-C4H8 ↔ C4H7•(1) + C4H7•(1)	14.1	−0.7	166
C2H6 + C2H4 ↔ C2H5• + C2H5•	15.4	−0.3	273
C2H4 + CH4 ↔ C2H5• + CH3•	11.3	1.1	287

[A: s^{-1} for monomolecular reactions and mol m^{-3} s^{-1} for bimolecular reactions; E_a: in kJ mol^{-1}]. Note: the kinetic parameters correspond to the high pressure limit values for the forward endothermic reactions and the modified Arrhenius equation is used for the reaction rate coefficient: $k = AT^n\exp(-(E_a/(RT)))$.

As stated earlier, the simulation results for the components of the C4-fraction could be improved. This fraction is valuable and, thus, important for steam cracking, because it can be used to produce gasoline (from butenes) and rubbers (from butadiene). The parity plot in Figure 4 shows that both 1-butene and 1-pentene are systematically underpredicted while butadiene is systematically overpredicted. The results from the rate of production analysis show that both 1-butene and 1-pentene are almost entirely formed via the β-scission of the 3-hexyl radical

$$C_6H_{13}^{\bullet}(3) \Leftrightarrow 1 - C_4H_8 + C_2H_5^{\bullet} \quad (6)$$

$$C_6H_{13}^{\bullet}(3) \Leftrightarrow 1 - C_5H_{10} + CH_3^{\bullet} \quad (7)$$

Both 1-butene and 1-pentene are partly converted to butadiene. Hydrogen abstraction from 1-butene leads to the formation of the allylic 1-buten-3-yl radical, while the C-H β-scission of the 1-buten-3-yl radical yields butadiene

$$C_4H_7^{\bullet} \Leftrightarrow C_4H_6 + H^{\bullet} \quad (8)$$

Table 5. Simulated Conversion and Product Yields for *n*-Hexane Steam Cracking with 3 Different Mechanisms

	Mechanism 1 (wt%)	Mechanism 2 (wt%)	Full Mechanism (wt%)
H_2-yield	0.4	0.4	0.4
CH_4-yield	6.2	5.9	6.0
C_2H_2-yield	0.2	0.2	0.2
C_2H_4-yield	19.3	20.3	19.0
C_2H_6-yield	2.8	2.7	2.7
C_3H_4-yield	0.2	0.2	0.2
C_3H_6-yield	10.7	9.6	10.4
C_4H_6-yield	4.7	4.2	4.4
1-C_4H_8-yield	4.3	5.2	4.4
2-C_4H_8-yield	1.7	1.0	1.8
1-C_5H_{10}-yield	1.1	1.0	1.1
C_6H_{14}-conversion	51.5	50.8	50.9

Mechanism 1: disproportionation reaction family not considered. Mechanism 2: hydrogen migration reaction family not considered. Full mechanism of 1178 reactions: all reaction families considered [simulation conditions: CIT = 873 K, COT = 997 K, CIP = 0.27 MPa, COP = 0.24 MPa; F: 4.0 kg h^{-1}, δ = 0.4 kg/kg].

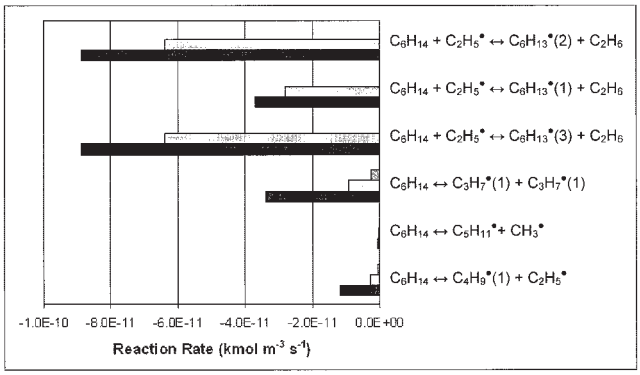

Figure 5. Comparison between reaction rates (kmol m^{-3} s^{-1}) of hydrogen abstraction reactions from n-hexane and C-C scissions of n-hexane.

Inlet: 0.0 m, middle: 6.2 m, outlet: 12.3 m.

Hydrogen abstraction from 1-pentene leads to the formation of the allylic 1-penten-3-yl $C_5H_9^{\bullet}$-radical, and the following β-scission of this radical forms butadiene

$$C_5H_9^{\bullet} \Leftrightarrow C_4H_6 + CH_3^{\bullet} \quad (9)$$

The rate constants for one or both of the reactions (Eq. 9) or (Eq. 10) may be too high in the model, but also our estimation of the thermochemistry of the 1-butene-3-yl radical or the 1-pentene-3-yl radical (since endothermic reactions (Eq. 9) and (Eq. 10) will be very sensitive to the thermochemistry as a consequence of the build-in thermodynamic consistency in RMG) can be responsible for the poor simulation results for butadiene. Indeed, model-predicted concentrations of many of the minor species, including butadienes, butanes, and pentenes, may depend strongly on the uncertain thermochemistry of resonance-stabilized radicals, as noted in Matheu et al.[63] Only a few of these radicals have well-established heats of formation and heat capacities (for example, allyl,[64] propargyl,[65,66] and cyclopentadienyl).[67,68] For the rest, including species like 1-butene-3-yl, even detailed, quantum-chemistry-based thermochemical estimates are fraught with uncertainty.[69,41]

The set of net pressure-dependent reactions reflecting the propargyl + propargyl, network and its associated isomerizations, based on the results of Miller and Klippenstein,[50] does not lead to the formation of a significant amount of benzene under the conditions used in this study. Addition reactions to olefinic products followed by cyclization reactions are probably more important for the formation of benzene, toluene and xylene under steam-cracking conditions at the lower conversions studied here (20–75% hexane conversion). However, both model and experiment agree that less than 1.0 of the hexane is converted into C6+ products at a total hexane conversion of 75%.

At the temperatures and pressures applied in steam cracking the thermodynamically favored products from those considered in the reaction network are clearly hydrogen and benzene. Even at low-temperatures of 600 K n-hexane will be completely converted at equilibrium. This is also shown from the estimated equilibrium concentrations calculated with the EQUIL tool from the CHEMKIN package.[42] The equilibrium concentrations for the main products at 1,000 K starting from pure n-hexane are: C_6H_6 20 mol %, H_2 80 mol %, CH_4 10^{-9} mol % and C_2H_4 10^{-8} mol %. Benzene can not be considered as the final product because benzene will ultimately form polycyclic aromatic hydrocarbons (PAH), and cokes via reactions omitted in this model.

Kinetic chain length

Two reaction families are equally important in determining the conversion of n-hexane: the hydrogen abstraction reactions and the C-C scission reactions of n-hexane. The hydrogen abstraction reactions convert n-hexane, while the C-C scission reactions and the recombination reactions determine the global radical concentration, and thus the concentration of β-radicals that can abstract hydrogen atoms from the feed molecules. The bar plot in Figure 5 shows that the reaction rates of the hydrogen abstractions from n-hexane are, apart from the inlet section, significantly faster than the rate of the C-C scission of n-hexane. This is further illustrated in Table 6, where the sum of the rates of all hydrogen abstraction reactions from n-hexane, and the sum of the rates of all C-C scission from n-hexane reactions are given as a function of the axial distance in the reactor. From the data presented in Table 6 the kinetic chain length at different axial positions can be calculated. The kinetic chain length is defined as the ratio of the rate of propagation to the rate of termination. In the steady state, the rate of initiation and the rate of termination are equal; hence, the kinetic chain length is equal to the ratio of the rate of propagation to the rate of initiation. The results in Table 6 show that initially the kinetic chain length is over 100, dropping to 80 in the middle of the reactor, while near the reactor outlet the kinetic chain length is slightly higher than 40. On average, a kinetic chain length of about 50 is found for an n-hexane conversion of 50%. For higher n-hexane conversions the average kinetic chain length drops to lower values.

μ-hypothesis and QSSA for μ-radicals

In industrial practice it is very important to determine modeling results as quickly as possible. This implies the implemen-

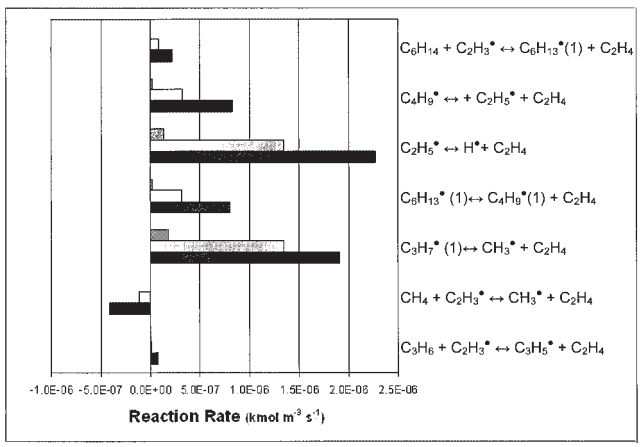

Figure 6. Bar plot showing the reaction rates for the important reactions involved in the formation and disappearance of ethylene.

Inlet: 0.5 m, middle: 6.2 m, outlet: 12.3 m.

Table 6. Values of the Reaction Rates for All C–C Scission Reactions and All Hydrogen Abstraction Reactions During the Cracking of Pure *n*-Hexane

	Reaction Rate (mol m^{-3} s^{-1})		
	5% Reactor Length	50% Reactor Length	95% Reactor Length
$\sum_i r_{i,\text{C–C scission reactions}}$	$3.42\ 10^{-1}$	$1.71\ 10^{-1}$	$5.45\ 10^{-2}$
$\sum_i r_{i,\text{Hydrgen abstractions}}$	65.05	14.83	2.39
Kinetic chain length	190	86	44

[$\sum_i r_{i,\text{C–C scission reactions}}$ the sum of the reaction rates of all C–C scission reactions of hexane; $\sum_i r_{i,\text{Hydrgen abstractions}}$ the sum of the reaction rates of the hydrogen abstraction reactions from *n*-hexane by all radicals].

tation of fast solvers, and encourages the use of models containing only a few species and reactions. However, as the average carbon number of the feedstock increases, the number of reactions and the number of species increases exponentially.[14] Therefore, modelers are always trying to reduce mechanisms, making them as compact as possible, and also to reduce the stiffness so the models can be solved more rapidly. A commonly applied assumption in modeling steam cracking and pyrolysis is the μ-hypothesis for large aliphatic radicals,[1,2,3] that is, bimolecular reactions are neglected for these radicals. These large radicals are called μ-radicals because they are involved in monomolecular reactions only. As stated earlier, in steam cracking radicals with more than five carbon atoms are considered μ-radicals.[1,2] Small radicals, such as the ethyl or propyl radical, are usually allowed to react by both unimolecular and bimolecular pathways. Benzyl and methyl radicals on the other hand are usually assumed to react only bimolecularly, that is, their unimolecular reactions are neglected ($\beta\mu$ rules of Goldfinger-Letort-Niclause[70]). RMG does not make any of these assumptions, hence, the generated reaction mechanism and the reduced mechanism for n-hexane can be used to check the validity of the μ-hypothesis. Our results indicate that the μ-hypothesis can indeed be used for large aliphatic radicals, as no bimolecular reactions of radicals with six or more carbon atoms are incorporated in the generated and reduced mechanisms by the RMG software (see Table 4) because these reactions are not fast enough during any time step to be included by the rate based criterion with the error tolerance applied in this work.

To overcome the stiffness problem of the continuity equations the radical concentrations are often computed using the quasi-steady-state approximation (QSSA).[71] There is some concern about the accuracy of this approximation, so in some modern steam cracking models the QSSA is only assumed to hold for the μ-radicals.[1,2] In this model the concentration of all species is calculated exactly using a stiff integrator, and KINALC[60] is used to estimate the errors introduced by applying the QSSA for each species in the reaction network. In Table 7 the lifetime and the instantaneous error from the quasi-steady-state approximation (QSSA) are given for some typical species in the reaction network. The latter is an indication of which species can be considered in the pseudo-steady-state.[72] If the continuity equations are written as

$$\frac{dc_i}{dt} = f_i(c_i, k_j') = -\sum_j \nu_{ij} R_j \tag{10}$$

the instantaneous error from the QSSA on the concentration of a single species Δc_i^s can be estimated by:

$$\Delta c_i^s = \frac{1}{J_{ii}} \frac{dc_i}{dt} \tag{11}$$

where

$$J_{ik} = \left[\frac{\partial f_i(\bar{c}, \bar{k})}{\partial c_k} \right]$$

The lifetime in the reactor is typically in the order of 10^{-1} s for molecules and 10^{-6} s for radicals. For larger radicals the lifetime is on average shorter, for example, for radicals with six or more carbon atoms the lifetime is in the order of 10^{-9} s (see Table 7). The results in Table 7 further show that the instantaneous error from applying the pseudo-steady state for all radicals is small, in particular for the radicals with five or more carbon atoms. Hence, these results give a first indication that the QSSA can be applied for the μ-radicals. The error resulting from the application of the QSSA to the group of μ-radicals can be calculated using the following equation[72]

$$\Delta c_i^g = \frac{1}{J_{ii}} \frac{dc_i}{dt} - \frac{1}{J_{ii}} \sum_{k \neq i} J_{ik} \Delta c_k^g \tag{12}$$

where i and k run over all QSS species in the group. The calculation of the group errors therefore requires the solution of

Table 7. Lifetimes and Estimated Single Quasi-Steady-State Species Error (Δc_i^s) in the Beginning and the Middle of the Reactor

	z_1 = 0.2 m		z_2 = 10 m	
	$\lvert\Delta c_i^s/c_i\rvert$	Lifetime (s)	$\lvert\Delta c_i^s/c_i\rvert$	Lifetime (s)
H_2	$6.68\ 10^{1}$	1.17	$1.02\ 10^{1}$	11.9
CH_4	$1.479\ 10^{2}$	2.53	$2.58\ 10^{1}$	19.1
C_2H_4	2.23	$3.80\ 10^{-2}$	0.14	0.12
C_3H_6	3.16	$5.58\ 10^{-2}$	0.18	0.15
C_4H_6	1.74	$1.12\ 10^{-2}$	0.12	$6.73\ 10^{-2}$
C_4H_8	1.46	$3.38\ 10^{-2}$	0.11	0.13
C_6H_{14}	0.99	$2.37\ 10^{-1}$	1.00	3.1
$H^{\bullet}$	$1.31\ 10^{-4}$	$7.86\ 10^{-9}$	$3.67\ 10^{-8}$	$6.90\ 10^{-9}$
$CH_3^{\bullet}$	$3.44\ 10^{-4}$	$2.27\ 10^{-6}$	$9.07\ 10^{-6}$	$2.25\ 10^{-6}$
$C_2H_3^{\bullet}$	$2.74\ 10^{-4}$	$2.66\ 10^{-7}$	$1.27\ 10^{-6}$	$3.76\ 10^{-7}$
$C_2H_5^{\bullet}$	$3.82\ 10^{-5}$	$2.31\ 10^{-7}$	$7.13\ 10^{-6}$	$3.32\ 10^{-6}$
$C_3H_5^{\bullet}$(al)	$1.46\ 10^{-3}$	$8.14\ 10^{-5}$	$1.40\ 10^{-4}$	$1.16\ 10^{-4}$
$C_4H_9^{\bullet}$(1)	$3.83\ 10^{-5}$	$2.60\ 10^{-10}$	$5.11\ 10^{-10}$	$7.45\ 10^{-9}$
$C_6H_{13}^{\bullet}$(1)	$1.71\ 10^{-5}$	$3.10\ 10^{-7}$	$1.81\ 10^{-6}$	$1.10\ 10^{-7}$
$C_6H_{13}^{\bullet}$(2)	$5.51\ 10^{-5}$	$3.34\ 10^{-9}$	$1.61\ 10^{-8}$	$7.75\ 10^{-9}$
$C_6H_{13}^{\bullet}$(3)	$5.56\ 10^{-5}$	$2.94\ 10^{-9}$	$1.97\ 10^{-8}$	$8.21\ 10^{-9}$

[Conditions z_1: T = 927 K, P = 0.21 MPa; Conditions z_2: T = 987 K, P = 0.19 MPa].

a coupled set of linear algebraic equations. If the group errors of all species remain small, then the chosen group of species can be considered as QSS species. In our case the group error for the group of radicals with five or more carbons atoms can be neglected. Hence, it can be concluded that in our case the QSSA for μ-radicals is valid.

Importance of pressure dependence

The effect of the pressure on the reaction-rate coefficient is usually neglected in steam cracking simulations. The available software programs (SPYRO,[73,74] CRACKER,[75] CRACKSIM[2,76]) neglect the pressure dependence of the rate coefficients. Dean et al.[28] and Grenda et al.[77] showed that the inclusion of pressure-dependence can be important for the pyrolysis of methane. Also for high-conversion ethane steam cracking,[29] oxidative coupling of methane[78] and methane autocatalysis[20] including pressure dependent pathways proved to be important, especially for an accurate prediction of the yields of the minor products. For reactions of large molecules (more than 8 –10 heavy atoms) the high-pressure limit approximation is almost always used in literature.[47,79] However, Wong et al.[27] suggested that this approximation might not be correct, and demonstrated that under standard steam cracking conditions some of the β-scission reactions can be pressure dependent, for example, the β-scission of a primary butyl radical forming an ethyl radical and ethylene. Their analysis of the molecular size dependence of falloff and chemical activation indicates that many types of reactions are pressure-dependent even for very large molecules and even under relatively high-pressure conditions. The question arises if the high-pressure limit approximation used in most steam cracking models could affect the predictions under typical conditions.

The current version of RMG generates two reaction networks: one reaction network where pressure dependence is taken into account, and another reaction network with the reaction rate coefficients fixed at the high-pressure limit. In all cases (including many commercial steam cracking models) pressure-dependence is included for a handful of small-molecule reactions, for example, $H+H+M=H_2+M$, whose rates are very well established. The unresolved issue is how to handle the more complicated chemically-activated reactions of larger molecules, where the true pressure-dependence is unknown, and it is challenging to compute the rates accurately. Note that the required computational cost, and the required detailed transition-state information for every elementary step in each pressure-dependent system, make the most accurate methods, such as an RRKM/master equation approach, impractical at present for on-line k(T,P) predictions. The CHEMDIS calculations used here to compute k(T,P) are typically within a factor of 3 of the most accurate methods for computing k(T,P), but are much faster and more easily automated.[20]

The difference between the yields calculated, based on the two reaction networks, makes it possible to estimate the overall effect of pressure dependence on the simulation results. In Table 8 the simulation results obtained with the two different reaction networks are given. It is clear that for the major products the differences are relatively unimportant. However, a small but significant difference is seen for the simulated ethylene yield. The pressure-dependence effects are expected to be much more important at extremely high conversions,[20,29] but apparently they are not very important at the more typical conversions used in commercial units. There are several reasons why for n-hexane cracking pressure dependence remains relatively unimportant. First, the effect of pressure dependence on the conversion is limited because the reactions strongly affecting the conversion, that is, C-C scission and hydrogen abstractions, are only slightly pressure dependent or are pressure independent. Wong et al.[27] reported that C-C molecular scissions are P-independent up to very high temperatures, while the hydrogen abstraction reactions are P-independent. Second, many of the strongly-pressure-dependent small-molecule reactions are partially equilibrated, hence, their exact rates are not important. This is the case for the β-scission reaction of the ethyl radical and the reverse addition reaction. Although k(T,P)/$k\infty$(T) equals 0.68 at 1,000 K for both the forward and reverse reaction and n-hexane conversion is quite sensitive to these reactions, the effect of pressure dependence on the conversion remains small. Also, the effect on the product yields is limited because the rate of most β-scission reactions of larger radicals is high resulting in the absence of competitive reaction pathways. Even if the main pathway's rate is changed by a factor of 2, the product distribution would not be significantly affected. Moreover, the different β-scission reactions of a larger radical all have similar pressure dependence, hence weakening the effect of pressure on the product distribution even more.

Table 8. Simulated Conversion and Product Yields for *n*-Hexane Steam Cracking with the High Pressure Limit Mechanism (Kinetic Parameters in the High Pressure Limit) and Pressure Dependent Mechanism (Pressure Dependent Kinetic Parameters)

	High-Pressure Limit Mechanism (wt%)	Pressure Dependent Mechanism (wt%)
H_2-yield	0.4	0.4
CH_4-yield	5.9	6.0
C_2H_2-yield	0.3	0.2
C_2H_4-yield	19.5	19.0
C_2H_6-yield	2.7	2.7
C_3H_4-yield	0.2	0.2
C_3H_6-yield	10.7	10.4
C_4H_6-yield	4.1	4.4
1-C_4H_8-yield	4.4	4.4
2-C_4H_8-yield	1.8	1.8
1-C_5H_{10}-yield	1.0	1.1
C_6H_{14}-conversion	51.1	50.9

[Simulation conditions: CIT = 873 K, COT = 997 K, CIP = 2.7 MPa, COP = 2.4 MPa; F: 4.0 kg h^{-1}, δ = 0.4 kg/kg].

As stated earlier, n-hexane can be considered a model compound for naphtha steam cracking. Light and heavy naphthas are the most commonly applied hydrocarbon feedstocks in industrial steam cracking installations, for example, in Europe and Asia more than 90% of the steam cracking feeds are naphtha feedstocks. The conclusions found in this work for n-hexane cracking will most probably also hold for naphtha steam cracking. While neglecting pressure-dependence in naphtha steam-cracking leads to small but noticeable errors on the product yields, it appears that the high-pressure limit approximation commonly applied in simulation packages for steam cracking of complex mixtures is sufficiently accurate for most practical purposes.

Conclusions

A new network generator, RMG, is used to automatically generate a pressure-dependent reaction mechanism for the steam cracking of n-hexane. The RMG generated mechanism at constant temperature, pressure and volume is used in combination with CHEMKIN's PLUG utility to simulate the experiments performed in the pilot plant installation of the Laboratorium voor Petrochemische Techniek (LPT) in Ghent University. The simulations are in excellent agreement with experimental data obtained from the pilot plant. This is especially remarkable because none of the kinetic parameters used for generating the mechanism and obtaining the simulation results were fitted to the experimental data. The results for some minor products, such as 1-butene, 1-pentene and butadiene could be improved, but these predictions depend both on specific, uncertain rate rules and on poorly-established thermochemistry estimates for resonance-stabilized radicals. A more detailed kinetic database or more accurate thermochemical data could improve the agreement with the experimental data obtained from the pilot plant. This seems especially important for the accuracy of the simulated C4-fraction. At higher conversions the differences become even more significant. This effect could be attributed to new reaction paths and species that become important as the conversion increases, for example, paths consuming light olefins and forming benzene and toluene. Again, many of these reactions depend on uncertain radical thermochemistry and reaction rate estimates.

The results from the sensitivity and rate of production analysis show that although rate based construction of reaction mechanisms leads to smaller mechanisms than some other automated mechanism generation algorithms, a large number of unnecessary reactions is still included in the full mechanism. A compact mechanism of less than 100 reactions is adequate for simulating n-hexane steam cracking. The reduced mechanism shows that hydrogen migration reactions are of little importance, although they slightly affect the yields of ethylene, propylene, and the internal distribution of the C4-fraction. Other reaction families, such as the disproportionation reactions do not seem to be of any importance under typical steam cracking conditions. The sensitivity analysis performed on the kinetic rate rules shows that the accurate quantitative simulation results for n-hexane steam cracking depend strongly on the accuracy of the bond scission rate rules.

Generating a reaction mechanism for n-hexane using RMG verifies the μ-radical hypothesis. RMG does not consider any assumption to generate a detailed reaction mechanism, and is, hence, an excellent tool to test this and other assumptions employed in conventional modeling. Under our conditions these hypotheses as applied in steam cracking, that is, bimolecular reactions involving radicals with more than 5 carbon atoms are not fast compared to unimolecular reaction possibilities and can hence be neglected, is indeed valid. Also the QSSA for the radicals has been tested, in particular the error resulting from assuming the quasi steady state for the group of μ-radicals. Our results obtained with KINALC[60] show that the error for applying the quasi-steady state for the group of μ-radicals is negligible.

An indication of the effect of pressure dependence of the rate coefficients can also be obtained using RMG. In our case the effect of pressure dependence on the predicted conversion and the yields of the major products is limited. This implies that the assumption used in many simulation programs for naphtha cracking — that all potentially pressure-dependent reactions are in the high-pressure limit — does not strongly perturb predicted yields and product distributions. However, prior work indicates that pressure dependence becomes more important as the conversion increases.

Acknowledgments

Kevin M. Van Geem holds a PhD grant of the Institute for the Promotion of Innovation by Science and Technology in Flanders (IWT-Vlaanderen). Development of the RMG software package was made possible through financial support from the U.S. National Science Foundation under Grant No. 0312359 and from the U.S. Department of Energy under Grant DE-FG02-98ER14914.

Notation

c_j = concentration of species jmol m^{-3}
CIP = coil inlet pressure, MPa
CIT = coil inlet temperature K
COP = coil outlet pressure, MPa
COT = coil outlet temperature, K
F = flow rate, kg h^{-1}
k = reaction-rate coefficient variable
$k\infty$ = reaction-rate coefficient for P$\rightarrow\infty$ variable
l = reactor length, m
P = pressure, MPa
R = reaction rate, mol m^{-3} s^{-1}
r_j = net production rate of species jmol m^{-3} s^{-1}
T = process gas temperature K
X = conversion %
(al) = allylic carbon atom
(i) = radical carbon atom, i
(v) = vinylic carbon atom

Greek Symbols

δ = steam to hydrocarbon dilution
θ = residence time, s

Literature Cited

1. Ranzi E, Dente M, Plerucci S, Biardi G. Initial product distribution from pyrolysis of normal and branched paraffins. *Ind & Eng Chem Fund*. 1983;22(1):132-139.
2. Clymans PJ, Froment GF. Computer generation of rate equations in the thermal cracking of normal and branched paraffins. *Comp Chem Eng*. 1984;8:137-142.
3. Warth V, Stef N, Glaude PA, Battin-Leclerc F, Scacchi G, Côme GM. Computer-aided derivation of gas-phase oxidation mechanisms: Application to the modeling of the oxidation of n-butane. *Combustion & Flame*. 1998;114:81-102.
4. Chinnick SJ, Baulch DL, Ayscough PB. An expert system for hydrocarbon pyrolysis reactions. *Chemometrics and Intelligent Laboratory Systems*. 1988;5:39.
5. Hillewaert LP, Diericks JL, Froment GF. Computer-generation of reaction schemes and rate-equations for thermal-cracking. *AIChE J.* 1988;34:17.
6. Chevalier C, Warnatz J, Melenk H. Automatic generation of reaction-mechanisms for the description of the oxidation of higher hydrocarbons. *Ber Buns Phys Chem.* 1999;94(11):1362-1367.
7. Froment GF. *Chemical Reactions in Complex Systems*: the Mobil Workshop, A V Sapre and F J Krambeck, New York: Van Nostrand Reinhold; 1991.
8. DiMaio FP, Lignola PG. KING, a Kinetic network generator. *Chem Eng Sci*. 1992;47:2713.
9. Quann RJ, Jaffe SB. Structure-oriented lumping - Describing the chemistry of complex hydrocarbon mixtures. *Ind Eng Chem Res*. 1992;31(11):2483-2497.

10. Blurock ES. Reaction - system for modeling chemical reactions. *J Chem Inf Comp Sci*. 1995;35:607.
11. Ranzi E, Faravelli T, Gaffuri P, Sogaro A. Low temperature combustion - automatic-generation of oxidation reactions and lumping procedures. *Combustion & Flame*. 1995;102(1-2):179-192.
12. Broadbelt LJ, Stark SM, Klein MT. Computer-generated pyrolysis modeling - on-the-fly generation of species, reactions, and rates. *Ind Eng Chem Res*. 1994;33(4):790-799.
13. Prickett SE, Mavrovouniotis ML. Construction of complex reaction systems. *Comp Chem Eng*. 1997;21:1219-1325.
14. Susnow RG, Dean AM, Green WH, Peczak P, Broadbelt LJ. Rate-based construction of kinetic models for complex systems. *J Phys Chem A*. 1997;101:3731.
15. Warth V, Battin-Leclerc F, Fournet PA, Glaude PA, Côme GM, Scacchi G. Computer based generation of reaction mechanisms for gas-phase oxidation. *Comp Chem*. 2000;24:541.
16. Battin-Leclerc F, Glaude PA, Warth V, Fournet R, Scacchi G, Come GM. Computer tools for modelling the chemical phenomena related to combustion. *Chem Eng Sci*. 2000;55:2883.
17. Broadbelt LJ, Stark SM, Klein MT. Termination of computer-generated reaction-mechanisms - Species rank-based convergence criterion. *Ind Eng Chem Res*. 1995;34(8):2566-2573.
18. Broadbelt LJ, Stark SM, Klein MT. Computer generated reaction modeling: decomposition and encoding algorithms for determining species uniqueness. *Comp Chem Eng*. 1996;20:113.
19. Matheu DM, Green WH, Grenda JM. Capturing pressure-dependence in automated mechanism generation: Reactions through cycloalkyl intermediates. *Int J Chem Kin.* 2003[a];35:95-119.
20. Matheu DM, Dean AM, Grenda JM, Green WH. Mechanism generation with integrated pressure dependence: A new model for methane pyrolysis. *J Phys Chem A*. 2003[c];107:8552-8565.
21. Song J, Raman S, Yu J, Wijaya CD, Stephanopoulos G, Green WH, RMG: the Next Generation of Automatic Chemical Reaction Mechanism Generator. proceedings *AIChE Annual Meeting*. San Francisco, CA, USA; 2003.
22. Song J.. Massachusetts Institute of Technology, 2004. PhD Dissertation
23. Froment GF. Kinetics and Reactor Design in the Thermal Cracking for Olefin Production. Chem. Eng. Sci. 1992;47:2163.
24. Van Geem KM, Reyniers MF, Marin GB. Two severity indices for scale-up of steam cracking coils. *Ind Eng Chem Res*. 2005;44(10): 3402-3411.
25. Gavalas GR. The long chain approximation in free radical reaction systems. *Chem Eng Sci*. 1966;21:133-144.
26. LaMarca C, Linanati C, Klein MT. Design of kinetically coupled Complex Reaction Systems. Chem. Eng. Sci. 1990;45(8):2059-2065.
27. Wong BM, Matheu DM, Green WH. Temperature and molecular size dependence of the high-pressure limit. *J Phys Chem A*. 2003;107: 6206-6211.
28. Dean AM, Detailed kinetic modeling of autocatalysis in methane pyrolysis. *J Phys Chem*. 1990;94.
29. Matheu DM, Saeys M, Grenda JM, Marin GB, Green WH. New Models and Pathways for Methane and Ethane Pyrolysis from Automated, Pressure-Dependent Mechanism Generation. AIChE Annual meeting. San Francisco, CA, USA, 2003.
30. Matheu DM, Grenda JM, Saeys M, Green WH. New, computer-discovered pathways for methane and ethane pyrolysis. Preprints of the ACS Division of Fuel Chemistry; 2003[d].
31. Zajdlik R, Reyniers MF, Marin GB. Steam Cracking of Hydrocarbons in a Pilot Plant. AIChE Spring meeting. New Orleans; 2003.
32. Wauters S, Marin GB. Kinetic modeling of coke formation during steam cracking. *Ind Eng Chem Res*. 2002;41:2379-2391.
33. Reyniers MF, Froment GF. Influence of metal surface and sulfur addition on coke deposition in the thermal cracking of hydrocarbons. *Ind Eng Chem Res*. 1995;34:773-785.
34. Dhuyvetter I, Reyniers MF, Froment GF, Marin GB. The influence of dimethyl disulfide on naphtha steam cracking. *Ind Eng Chem Res*. 2001;40:4353-4362.
35. Van Damme PS, Froment GF. Putting computers to work - Thermal cracking computer control in pilot plants. *Chem Eng Progr*. 1982; 78(9):77-82.
36. Wijaya CD. Massachusetts Institute of Technology; 2005. PhD Dissertation.
37. Benson SW. Thermochemical Kinetics. 2nd ed. New York, John Wiley & Sons, Inc; 1976.
38. Lay TH, Bozzelli JW, Dean AM, Ritter ER. Hydrogen atom bond increments for calculation of thermodynamic properties of hydrocarbon radical species. *J Phys Chem*. 1995;99(39):14514-14527.
39. Sumathi R, Green WH. A priori rate constants for kinetic modeling. *Theoretical Chemistry Accounts*. 2002[a];108:187-213.
40. Sumathi R, Green WH. Missing thermochemical groups for large unsaturated hydrocarbons: Contrasting predictions of G2 and CBS-Q. *J Phys Chem*. A. 2002;106(46):11141-11149.
41. Sumathi R, Green WH. Oxygenate, oxyalkyl, and alkoxycarbonyl thermochemistry and rates for hydrogen abstraction from oxygenates. *Phys Chem Chem Phys*. 2003;5:3402-3417.
42. Kee RJ, Rupley FM, Miller JA, Coltrin ME, Grcar JF, Meeks E, Moffat HK, Lutz, G Dixon-Lewis AE, Smooke MD, Warnatz J, Evans GH, Larson RS, Mitchell RE, Petzold LR, Reynolds WC, Caracotsios M, Stewart WE, Glarborg P, Wang C, Adigun O, Houf WG, Chou CP, Miller SF, Ho P, Young DJ. CHEMKIN Release 401. Reaction Design Inc. CA: San Diego; 2004.
43. Sumathi R, Carstensen HH, Green WH. Reaction rate prediction via group additivity, Part 1: H abstraction from alkanes by H and CH_3. *J Phys Chem A*. 2001[a];105:6910-6925.
44. Sumathi R, Carstensen HH, Green WH. Reaction rate prediction via group additivity, Part 2: H abstraction from alkenes, alkynes, alcohols and acids by H atoms. *J Phys Chem A*. 2001;105:8969-8984.
45. Wijaya CD, Sumathi R, Green WH. Cyclic ether formation from hydroperoxyalkyl radicals (QOOH). *J Phys Chem A*. 2003;107:4908-4920.
46. Saeys M, Reyniers MF, Marin GB, Van Speybroeck V, Waroquier M. Ab Initio Group Contribution Method for Activation Energies for Radical Additions. *AIChE J*. 2004;50(2):426-444.
47. Curran HJ, Gaffuri P, Pitz WJ, Westbrook CK. A comprehensive modeling study of n-heptane oxidation. *Combustion & Flame*. 1998; 114:149.
48. Chang, AY, Bozzelli JW, Dean AM. Kinetic Analysis of Complex Chemical Activation and Unimolecular Dissociation Reactions using QRRK Theory and the Modified strong Collision Approximation. Z. Phys. Chem. 2000; 214:1533-1568.
49. Matheu DM, Lada TA, Green WH, Grenda JM, Dean AM. Rate-based screening of pressure-dependent reaction networks. *Comp Phys Comm*. 2001;138:237-249.
50. Miller JA, Klippenstein SJ. The recombination of propargyl radicals and other reactions on a C_6H_6 potential. *J Phys Chem A*. 2003;107: 783-7799.
51. Li S, Petzold LR. *Design of New DASPK for Sensitivity Analysis*. UCSB Technical report;1999.
52. Song J, Stephanopoulos G, Green WH. Valid parameter range analyses for Chemical Reaction Kinetic Models. Chem. Eng. Sci. 2002; 57: 4475-4491.
53. Bozzelli JW, Chang AY, Dean AM. Molecular density of states from estimated vapor phase heat capacities. *Int J Chem Kin*. 1997;29:161-170.
54. Van Geem KM, Heynderickx GJ, Marin GB. A Comparison of one and two-dimensional reactor models for steam cracking: Effect on yields and coking rate. *AIChE J*. 2004[a];50:173-183.
55. Caracotsios M, Stewart WE. Sensitivity analysis of initial-value problems with mixed ODES and algebraic equations. *Comp Chem Eng*. 1985;9(4):359-365.
56. Turanyi T. Sensitivity analysis of complex kinetic systems. Tools and applications. *J Math Chem*. 1990;5:203-204.
57. Turanyi T, Berces T, Vajda S. Reaction-rate analysis of complex kinetic systems. *Int J Chem Kin*. 1989;21(2):83-99.
58. Rota R, Bonini F, Servida A, Morbidelli M, Carra S. Validation and updating of detailed kinetic mechanisms: The case of ethane oxidation. *Ind Eng Chem Res*. 1994;33:2540-2553.
59. Brock EE, Savage PE, Barker JR. A Reduced mechanism for methanol oxidation in supercritical wate. *Chem Eng Sci*. 1998;53(5):857-867.
60. Turanyi T. Applications of sensitivity analysis to combustion chemistry. *Reliability Eng & System Safety*. 1997;57(1):41-48.
61. Tomlin AS, Pilling MJ, Merkin JH, Frindley J, Burgess N, Gough A. Reduced mechanism for propane pyrolysis. *Ind Eng Chem Res*. 1995; 34:3749-3760.
62. Van Damme PS, Willems PA, Froment GF. Temperature, not time, controls steam cracking yields. *Oil & Gas J*. 1984;68-73.

63. Matheu DM, Grenda JM. A Systematically-generated, pressure-dependent mechanism for high-conversion ethane yrolysis Part I: Pathways to the minor products. *J. Phys Chem A*. 2005;109(24):5332-5342.
64. Wenthold PG, Polak ML, Lineberger WC. Photoelectron spectroscopy of the allyl and 2-methylallyl anions. *J Phys Chem*. 1996;100(17): 6920-6926.
65. Afeefy HY, Liebman JF, Stein SE. Neutral Thermochemical Data: In NIST Chemistry Webbook, NIST Standard Reference Database Number 69, Linstrom PJ; Mallard WG. eds. MD:Gaithersburg; 2001.
66. Sabbe MK, Saeys M, Reyniers MF, Marin GB. Group additive values for the gas phase standard enthalpy of formation of hydrocarbons and hydrocarbon radicals. *J Phys Chem. A*. 2005 (accepted).
67. Roy K, Braun-Unkhoff M, Frank P, Just T. Kinetics of the cyclopentadiene decay and the recombination of cyclopentadienyl radicals with H-atoms: Enthalpy of formation of the cyclopentadienyl radical. *Int J Chem Kin*. 2001;33(12):821-833.
68. Kiefer JH, Tranter RS, Wang H, Wagner AF. Thermodynamic functions for the cyclopentadienyl radical: The effect of Jahn-Teller distortion. *Int J Chem Kin*. 2001;33 (12):834-845.
69. Henry DJ, Parkinson CJ, Radom L. An assessment of the performance of high-level theoretical procedures in the computation of heats of formation of small open-shell molecules. *J Phys Chem A*. 2002;106: 7927-7936.
70. Laidler KJ.*Chemical Kinetics.* 3rd ed. New York: Harper & Row; 1987.
71. Bodenstein M, Lutkemeyer H. Die photochemische bildung von brommwasserstoff und die bildungsgeschwindigkeit der brommolekel aus den atomen. *Z Phys Chem*. 1924;114:208.
72. Turanyi T, Tomlin AS, Pilling MJ. On the error of the quasi-steady-state approximation *J Phys Chem*. 1993;97(1):163-172.
73. Van Goethem MWM, Kleinendorst FI, Van Leeuwen C, Van Velzen N. Equation-based SPYRO® model and solver for the simulation of the steam cracking process. *Comp Chem Eng*. 2001;25:905-911.
74. Dente M, Ranzi E, Goossens AG. Detailed prediction of olefin yields from hydrocarbon pyrolysis trough a fundamental simulation-model (SPYRO). *Comp Chem Eng*. 1979;3:61-75.
75. Joo E, Lee K, Lee M, Park S. CRACKER - a PC Based simulator for industrial cracking furnaces. *Comp Chem Eng*. 2000;24:1523-1528.
76. Van Geem KM, Reyniers MF, Marin GB. First Principles based Reaction Network for Steam Cracking, AIChE Annual Meeting, TX: Austin; 2004b.
77. Grenda JM, Androulakis IP, Dean AM, Green WH. Application of computational kinetic mechanism generation to model the autocatalytic pyrolysis of methane. *Ind Eng Chem Res*. 2003;42(5):1000-1010.
78. Chen Q, Couwenberg PM, Marin GB. Effect of pressure on the oxidative coupling of methane in the absence of catalyst. *AIChE J*. 1994;40(3):521-535.
79. Larson CW, Patrick R, Golden DM. Pressure and temperature-dependence of unimolecular bond fission reactions - an Approach for combustions modelers. *Combustion & Flame*. 1984;58:229.

Manuscript received May 3, 2005, and revision received July 6, 2005.